An Improved Principal Coordinate Frame for use with Spatial Rigid Body Displacement Metrics

Pierre Larochelle[1] and Venkatesh Venkataramanujam[2]

[1] South Dakota School of Mines & Technology, Rapid City SD 57701, USA,
Pierre.Larochelle@sdsmt.edu,
WWW home page: http:larochelle.sdsmt.edu/
[2] SoftBank Robotics, Boston, MA 01864, USA,
vvenkata@hotmail.com,
WWW home page: https://www.softbankrobotics.com/

Abstract. This paper presents an improved definition of a coordinate frame, entitled the principal frame (PF), that is useful for metric calculations on spatial rigid-body displacements. For a finite set of displacements a point mass model of the moving rigid-body is employed. Next, we compute the centroid and principal axes associated with the point mass locations. The PF is then determined from the principal axes. Here, a new algorithm for determining the PF from the principal axes is proposed. The PF is invariant with respect to the choice of the fixed coordinate frame as well as the system of units used; therefore, the PF is useful for left invariant metric computations. An example including a set of 10 spatial rigid-body displacements is presented to demonstrate the application and utility of the PF.

Keywords: displacement metrics, rigid-body displacements, SE(3)

1 Introduction

This paper presents a new procedure, which directly builds upon prior work reported in [1, 2], for identifying a useful fixed frame to perform metric computations on finite sets of spatial displacements. A metric is used to measure the distance between two points in a set. There are various metrics for finding the distance between two points in Euclidean space. However, finding the distance between two locations of a rigid-body, i.e. two elements of SE(3), is still the subject of ongoing research, see [1, 3–20]. Kazerounian and Rastegar [17] define metrics that depend upon the shape and mass density of the finite moving body. More recently, Angeles has investigated the use of characteristic lengths that are used to combine translations and rotations in some manner for use in distance metrics [19]. Finally, Di Gregorio [21] has sought to employ a geometric approach to identify useful distance metrics.

All metrics on the group SE(3) of spatial displacements yield a distance that is dependent upon the chosen fixed or moving frames of reference and the units used [9, 11]. Nevertheless, a metric independent of these choices, referred to as

T. Uhl (ed.), *Advances in Mechanism and Machine Science*,
Mechanisms and Machine Science 73,
https://doi.org/10.1007/978-3-030-20131-9_32

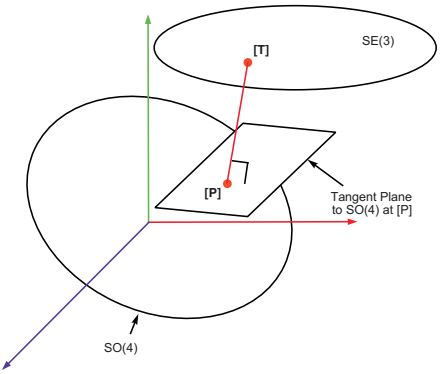

Fig. 1. SE(3) to SO(4)

bi-invariant, is desirable. Metrics independent of the choice of coordinate frames and the units used do exist on SO(N), Larochelle [12]. One bi-invariant metric defined by Ravani and Roth [22] defines the distance between two orientations of a rigid-body as the magnitude of the difference between the associated quaternions. Of related background interest are the works by Horn [23] and Shoemake and Duff [24]. Horn solved the problem of finding the rigid-body transformation between two coordinate frames using point coordinates using Hamilton's quaternions whereas Shoemake and Duff examined the problem of decomposing homogeneous rigid-body displacements into rotations and translations using the polar decomposition.

The PF has been introduced to support the use of polar decomposition based metrics on the spatial displacement group [1, 2, 26, 25]. These techniques are based on the polar decomposition (PD) of the homogenous transform representation of the elements of SE(3) and the principal frame PF associated with the finite set of rigid-body displacements. The mapping of the elements of the special Euclidean group SE(3) to SO(4) yields hyper-dimensional rotations that approximate the rigid-body displacements. Conceptual representations of the mapping of SE(3) to SO(4) are shown in Figures 1 and 2; note the axis coloring convention that is used throughout the paper: red $= x$ axis, green $= y$ axis, and blue $= z$ axis. Once the elements are mapped to SO(4) distances can then be evaluated by using a bi-invariant metric on SO(4). The use of the PF yields a metric on SE(3) that is left invariant, i.e. independent of the choice of the fixed reference frame.

2 The Polar Decomposition and a Metric on SO(4)

Here we briefly review the use of the polar decomposition on elements of SE(3) to yield hyper-dimensional rotations, i.e. element sof SO(4), which approximate spatial displacements of a rigid-body. The elements of SO(4) are derived from

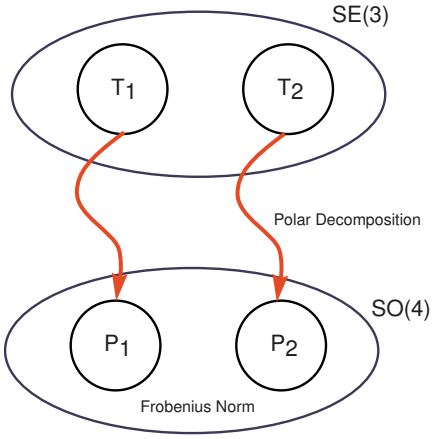

Fig. 2. Mapping to SO(4)

homogenous transformations representing spatial SE(3) displacements by polar decompositions as shown in Figure 2 and derived in [1, 2, 27]. A number of iterative algorithms exist for the evaluation of the polar decomposition. Higham described a method based upon Newtons Method, see [33]. A simple and efficient iterative algorithm for computing the polar decomposition is shown by Dubrulle [34]. The algorithm produces monotonic convergence in the Frobenius norm in ~ 10 or fewer steps. A MatLab implementation of the algorithm is shown below.

```
%% Dubrulle's Algorithm
%% Input T : Scaled transformation matrix in SE(3)
%% Output P : Projection in SO(4)
function P = polarmetric(T)
%Initialization
P = T;
limit = (1+eps)* sqrt(size(T,2));
T = inv(P');
g = sqrt(norm(T,'fro')/norm (P,'fro'));
P = 0.5*(g*P+(1/g*T));
f = norm(P,'fro');
pf = inf;
% Iteration
while (f>limit) & (f<pf)
    pf = f;
    T = inv(P');
    g= sqrt(norm(T,'fro')/f);
    P = 0.5*(g*P+(1/g*T));
    f = norm(P,'fro');
```

```
end
return
```

The distance between any two elements $[A_1]$ and $[A_2]$ in SO(4) is determined by using the Frobenius norm as follows,

$$d = \|[I] - [A_2][A_1]^T\|_F \tag{1}$$

See [28] for a proof that this is a valid metric on SO(N).

3 Conceptual Overview

The preceding section summarized the use of the polar decomposition to yield elements of SO(4) that approximate elements of SE(3). An additional challenge remains; the application of a metric on SO(N), i.e. on the approximating hyper-rotations, will not be well-defined because of the dependence on the choice of fixed reference frame. In order to mitigate this challenge and yield a useful metric on a finite set of spatial displacements the principal frame PF is introduced. The PF is unique for a finite set of displacements and invariant with respect to the choice of fixed coordinate frame and the system of units, see [29, 30]. All of the displacements are then expressed with respect to the principal frame and all distances are measured with respect to this same frame. Hence, the polar decomposition based metric yields results that are invariant with respect to the choice of fixed frame. Next, we present the detailed implementation of this methodology.

4 Determining the Principal Frame

Given a finite set of n spatial displacements we seek to determine their magnitudes. The displacements depend on the fixed and moving coordinate frames as well as the system of units employed. In order to yield a left invariant metric we utilize a PF that is derived from a unit point mass model for a moving body as suggested by [27, 4]. A unit point mass is assigned to the origin of each of the coordinate frames representing rigid-body displacements. The point masses are then used to determine the system's center of mass and, eventually the invariant principal frame of the set of displacements. This is done to yield a metric that is independent of the moving body's geometry and mass distribution. The center of mass and the PF are unique for the system and invariant with respect to both the choice of the fixed coordinate frame and the system of units [29, 30].

The procedure for determining the center of mass $\overrightarrow{c}$ and the PF associated with the n prescribed spatial locations is now described. A unit point mass is located at the origin of each location.

$$\overrightarrow{c} = \frac{1}{n}\sum_{i=1}^{n} \overrightarrow{d_i} \tag{2}$$

where, $\overrightarrow{d_i}$ is the translation vector associated with the i^{th} location, i.e. the origin of the i^{th} location with respect to the fixed frame.

The PF is defined such that its axes are aligned with the principal axes of the n point mass system and its origin is at the centroid $\overrightarrow{c}$. After finding the centroid of the system we determine the principal axes of the point mass system as follows. The inertia tensor is computed from,

$$[\mathrm{I}] = [1] \sum_{i=1}^{n} \|\mathbf{d}_i\|^2 - \sum_{i=1}^{n} \mathbf{d}_i \mathbf{d}_i^T \tag{3}$$

where [1] is the 3×3 identity matrix. The principal frame is then determined to be

$$[PF] = \begin{bmatrix} \overrightarrow{v_1} & \overrightarrow{v_2} & \overrightarrow{v_3} & \overrightarrow{c} \\ 0 & 0 & 0 & 1 \end{bmatrix} \tag{4}$$

where, $\overrightarrow{v_i}$ are the principal axes, i.e. the eigenvectors, associated with the inertia tensor [I], see Greenwood [29].

The directions of the vectors along the principal axes $\overrightarrow{v_i}$ are chosen such that the principal frame is a right-handed system. However, Equation (4) does not uniquely define PF since the eigenvectors $\overrightarrow{v_i}$ of the inertia tensor are not unique; i.e. both $\overrightarrow{v_i}$ and $-\overrightarrow{v_i}$ are eigenvectors associated with [I]. In order to resolve this ambiguity and yield a unique PF we chose the eigenvector directions that most closely aligns the PF with respect to the fixed frame. The three eigenvectors define 3 mutually orthogonal lines in space and are shown as black lines in Figure 3. For each octant of Figure 3 there are three possible definitions of the PF due to the 3 possible right-handed cyclic permutations of the x, y, and z axes. Therefore there are 24 different right-handed PF orientations associated with the three eigenvectors identified in Table 4. Note that each row of Table 4 is associated with one octant and therefore represents three possible orientations of the PF. For example, from Row 1, the three possible orientations of the PF are: $[\overrightarrow{v_1} \quad \overrightarrow{v_2} \quad \overrightarrow{v_3}]$, $[\overrightarrow{v_3} \quad \overrightarrow{v_1} \quad \overrightarrow{v_2}]$, and, $[\overrightarrow{v_2} \quad \overrightarrow{v_3} \quad \overrightarrow{v_1}]$. The PF is selected as the frame

Table 1. The 8 Octants Associated with the Eigenvectors

Octant	x axis	y axis	z axis
1	$\overrightarrow{v_1}$	$\overrightarrow{v_2}$	$\overrightarrow{v_3}$
2	$\overrightarrow{v_2}$	-$\overrightarrow{v_1}$	$\overrightarrow{v_3}$
3	-$\overrightarrow{v_1}$	-$\overrightarrow{v_2}$	$\overrightarrow{v_3}$
4	-$\overrightarrow{v_2}$	$\overrightarrow{v_1}$	$\overrightarrow{v_3}$
5	$\overrightarrow{v_2}$	$\overrightarrow{v_1}$	-$\overrightarrow{v_3}$
6	$\overrightarrow{v_1}$	-$\overrightarrow{v_2}$	-$\overrightarrow{v_3}$
7	-$\overrightarrow{v_2}$	-$\overrightarrow{v_1}$	-$\overrightarrow{v_3}$
8	-$\overrightarrow{v_1}$	$\overrightarrow{v_2}$	-$\overrightarrow{v_3}$

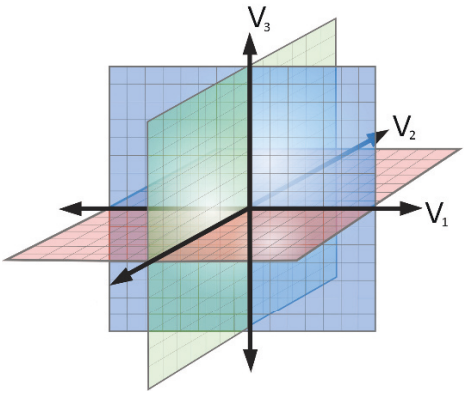

Fig. 3. The 8 Octants Associated with the Eigenvectors

that is most closely oriented, per Equation (1), to the fixed frame. However, there are degenerate cases that must now be addressed.

In the degenerate spatial case in which the lines defining the PF form equal angles with the axes of the fixed frame, there will be eight possible orientations that are equidistant to the fixed frame's orientation. In this case, the eigenvectors form equal angles (i.e. 54.7 deg) with each axis of the fixed frame so we define the x axis of the PF along the eigenvector in the first octant of the fixed reference frame and the y and z axes are chosen such that the PF is the frame that is most closely oriented, per Equation (1), to the fixed frame.

4.1 Normalizing the Translation Components

The unit disparity between translation and rotation is resolved by normalizing the translational terms in the displacements. The displacements are normalized by choosing a characteristic length R. The characteristic length used, based upon the investigations reported in [12, 32], is $\frac{24L}{\pi}$, where L is the maximum translational component in the set of displacements at hand. This characteristic length is the radius of the hypersphere that approximates the translational terms by angular displacements that are ≤ 7.5 degrees. It was shown in [32] that this characteristic length yields an effective balance between translational and rotational displacement terms for projection metrics. The metric presented here is therefore dependent on the choice of characteristic length. Note that larger characteristic lengths result in an increase in the weight on the rotational terms whereas smaller ones result in an increase in weight on the translational terms.

The elements of SE(3) are represented by,

$$T_i = \left[\begin{array}{c|c} [R] & \vec{t} \\ \hline 0\ 0\ 0 & 1 \end{array}\right] \tag{5}$$

where $[R]$ represents the rotational component and $\overrightarrow{t}$ represents the translational component of the homogenous transformation representation of the i^{th} location. The scaled transformation matrices are given by,

$$T_{i(scaled)} = \left[\begin{array}{ccc|c} & [R] & & \overrightarrow{t}/R \\ \hline 0 & 0 & 0 & 1 \end{array}\right] \tag{6}$$

where R represents the characteristic length used to resolve the unit disparity between rotation and translation. The scaled transformation matrices may then be mapped to SO(N) by using the Dubrulle algorithm for the polar decomposition.

4.2 Step by Step

For a set of n finite rigid-body spatial locations the steps to be followed are:

1. Determine the PF associated with the n locations.
2. Determine the relative displacements from the PF to each of the n locations.
3. Determine the characteristic length R associated with the n displacements with respect to the PF and scale the translation terms in each by $1/R$.
4. Compute the projections of PF and each of the scaled relative displacements using the polar decomposition.
5. The magnitude of the displacement is defined as the distance from the PF to the scaled relative displacement as computed via Equation (1). The distance between any two of the n locations is similarly computed by the application of Equation (1) to the projected scaled relative displacements.

5 Example

Consider the rigid-body guidance problem investigated by Larochelle [27]. The 10 spatial locations with respect to the fixed reference frame F are listed in Table 2/ The principal frame is given by,

$$[PF] = \begin{bmatrix} 0.756 & 0.000 & 0.655 & 5.500 \\ 0.000 & 1.000 & 0.000 & 0.000 \\ 0.655 & 0.000 & -0.756 & 0.000 \\ 0.000 & 0.000 & 0.000 & 1.000 \end{bmatrix}. \tag{7}$$

The maximum translational component L is found to be 6.7256 and the associated characteristic length is $R = \frac{24L}{\pi} = 51.3795$. The distance from the first location to the PF was found to be2.654. The distance between locations #1 and #2 was found to be 0.3485.

Table 2. Ten Desired Locations.

#	x	y	z	*Long* (θ)	*Lat* (ϕ)	*Roll* (ψ)
1	1.00	0.00	5.00	100	0.00	0.00
2	2.00	0.00	4.00	90	0.00	10.00
3	3.00	0.00	3.00	80	0.00	20.00
4	4.00	0.00	2.00	70	0.00	30.00
5	5.00	0.00	1.00	60	0.00	40.00
6	6.00	0.00	−1.00	50	0.00	50.00
7	7.00	0.00	−2.00	40	0.00	60.00
8	8.00	0.00	−3.00	30	0.00	70.00
9	9.00	0.00	−4.00	20	0.00	80.00
10	10.00	0.00	−5.00	10	0.00	90.00

6 Summary

This work presented an improved definition of a coordinate frame, entitled the principal frame (PF), which is useful for metric calculations on spatial rigid-body displacements. Though the PF was originally introduced in [1, 25, 26], presented here is an improved definition that yields the PF that is most closely oriented to the fixed reference frame. By using a point mass model for the moving rigid-body the PF is determined from the associated centroid and principal axes. The PF is left invariant, i.e. independent of both the choice of the fixed coordinate frame and the system of units used, therefore the PF is useful in performing left invariant distance metric computations on rigid-body spatial displacements. One example that utilized the PF and the polar decomposition based metric of Larochelle, Angeles, and Murray [2] was presented to demonstrate the utility of the PF. The PF has potential applications in the design of robotic mechanical systems; especially in motion synthesis and path generation.

7 Acknowledgments

We gratefully acknowledge the insightful discussions about metrics and the principal frame PF with Michal Juránek of Photoneo S.R.O. (https://www.photoneo.com). This work builds upon preliminary results reported in Refs. [1, 25, 2, 26].

References

1. Venkataramanujam, V., Larochelle, P.: A Coordinate Frame Useful for Rigid-Body Displacement Metrics. ASME J. Mechanisms and Robotics. vol. 2, no. 4 (2010). doi:10.1115/1.4002245
2. Larochelle, P., Murray, A., Angeles, J.: A Distance Metric for Finite Sets of Rigid-Body Displacements via the Polar Decomposition. ASME J. Mechanical Design. vol. 129, no. 8, pp. 805-812 (2006). doi:10.1115/1.2735640

3. Fanghella, P., Galletti, C.: Metric Relations and Displacement Groups in Mechanism and Robot Kinematics. ASME J. Mechanical Design. vol. 117, no. 3 (1995). doi:10.1115/1.2826702
4. Zefran, M., Kumar, V., Croke, C.: Metrics and Connections for Rigid-Body Kinematics. The Int. J. of Robotics Research. vol. 18, no. 2 (1999). doi:10.1177/027836499901800208
5. Park, F., Brocket, R.: Kinematic Dexterity of Robotic Mechanisms. The Int. J. of Robotics Research. vol. 13, no. 1 (1994). doi:10.1177/027836499401300101
6. Lin, Q., Burdick, J.: Objective and Frame-Invariant Kinematic Metric Functions for Rigid Bodies. The Int. J. of Robotics Research. vol. 19, no. 6 (2000). doi:10.1177/027836490001900605
7. Bobrow, J., Park, F.: On Computing Exact Gradients for Rigid Body Guidance Using Screw Parameters. In: Proceedings of the ASME Design Engineering Technical Conferences, vol. 1, pp. 839-844. ASME Press, New York (1995).
8. Chirikjian, G.: Convolution Metrics for Rigid Body Motion. In: Proceedings of the ASME Design Engineering Technical Conferences. ASME Press, New York (1998).
9. Park, F.: Distance Metrics on the Rigid-Body Motions with Application to Mechanism Design. ASME J. Mechanical Design. vol. 117, no. 1, pp. 48-54 (1995). doi:10.1115/1.2826116
10. Chirikjian, G., Zhou, S.: Metrics on Motion and Deformation of Solid Models. ASME J. Mechanical Design. vol. 120, no. 2, pp. 252-261 (1998). doi:10.1115/1.2826966
11. Martinez, J., Duffy, J.: On the Metrics of Rigid Body Displacements for Infinite and Finite Bodies. ASME J. Mechanical Design. vol. 117, no. 1, pp. 44-47 (1995). doi:10.1115/1.2826115
12. Larochelle, P., McCarthy, J.: Planar Motion Synthesis using an Approximate Bi-Invariant Metric. ASME J. Mechanical Design. vol. 117, no. 4, pp. 646-651 (1995). doi:10.1115/1.2826735
13. Etzel, C., McCarthy, J.: A Metric for Spatial Displacements Using Biquaternions on SO(4). In: Proceedings of IEEE International Conference on Robotics and Automation. vol. 4, pp. 3185-3190. IEEE International (1996). doi:10.1109/ROBOT.1996.509197
14. Gupta, K.: Measures of Positional Error for a Rigid Body. ASME J. Mechanical Design. vol. 119, no. 3, pp. 346-348 (1997).
15. Tse, D., Larochelle, P.: Approximating Spatial Locations With Spherical Orientations for Spherical Mechanism Design. ASME J. Mechanical Design. vol. 122, no. 4, pp. 457-463 (2000). doi:10.1115/1.1289139
16. Eberharter, J., Ravani, B.: Local Metrics for Rigid Body Displacements. ASME J. Mechanical Design. vol. 126, no. 5, pp. 805-812 (2004). doi:10.1115/1.1767816
17. Kazerounian, K., Rastegar, J.: Object Norms: A Class of Coordinate and Metric Independent Norms for Displacements. In: Proceedings of the ASME Design Engineering Technical Conferences, vol. 47, pp. 271-275. ASME Press, New York (1992).
18. Sharf, I., Wolf, A., Rubin, M.: Arithmetic and Geometric Solutions for Average Rigid-Body Rotation. Mechanism and Machine Theory. vol. 45, no. 9, pp. 1239-1251 (2010). doi:10.1016/j.mechmachtheory.2010.05.002
19. Angeles, J.: Is there a Characteristic Length of a Rigid-Body Displacement?. Mechanism and Machine Theory. vol. 41, no. 8, pp. 884-896 (2006). doi:10.1016/j.mechmachtheory.2006.03.010
20. Zhang, Y., Ting, K.: Point-Line Distance Under Riemannian Metrics. ASME J. Mechanical Design. vol. 130, no. 9, pp. 805-812 (2008). doi:10.1115/1.2943301

21. Di Gregorio, R.: A Novel Point of View to Define the Distance between Two Rigid-Body Poses. In: Lenarčič J., Wenger P. (eds) Advances in Robot Kinematics: Analysis and Design. Springer, Dordrecht (2008). doi:10.1007/978-1-4020-8600-7_38
22. Ravani, B., Roth, B.: Motion Synthesis Using Kinematic Mappings. ASME J. Mech., Trans., and Auto. vol. 105, no. 3, pp. 460-467 (1983). doi:10.1115/1.3267382
23. Horn, B.: Closed-Form Solution of Absolute Orientation using Unit Quaternions. J. of the Optical Society of America A. vol. 4, no. 4, pp. 629-642 (1987). doi: 10.1364/JOSAA.4.000629
24. Shoemake, K., Duff, T.: Matrix Animation and Polar Decomposition. In: Proceedings of Graphics Interface '92, pp. 258-264 (1992). doi:10.20380/GI1992.30
25. Venkataramanujam, V., Larochelle, P.: A Displacement Metric for Finite Sets of Rigid Body Displacements. In: Proceedings of the ASME Design Engineering Technical Conferences, vol. 2, pp. 1463-1469. ASME Press, New York (2008). doi:10.1115/DETC2008-49554
26. Venkataramanujam, V.: Approximate Motion Synthesis of Robotic Mechanical Systems. Masters thesis, Florida Institute of Technology (2007)
27. Larochelle, P.: A Polar Decomposition Based Displacement Metric for a Finite Region of SE(n). In: Lennarčič J., Roth B. (eds) Advances in Robot Kinematics. Springer, Dordrecht (2006). doi:10.1007/978-1-4020-4941-5_4
28. Schilling, R., Lee, H.: Engineering Analysis - A Vector Space Approach. Wiley, New York (2000). isbn:978-0471827603
29. Greenwood, D.: Advanced Dynamics. Cambridge University Press (2006). isbn: 978-0521029933
30. Angeles, J.: Fundamentals of Robotic Mechanical Systems. 4^{th} edition. Springer International Publishing (2014). isbn:978-3-319-01850-8
31. Al-Widyan, K., Cervantes-Sànchez, J., Angeles, J.: A Numerically Robust Algorithm to Solve the Five-Pose Burmester Problem. In: Proceedings of the ASME Design Engineering Technical Conferences. ASME Press, New York (2002).
32. Larochelle, P.: On the Geometry of Approximate Bi-Invariant Projective Displacement Metrics In: Proceedings of the World Congress on the Theory of Machines and Mechanisms (1999).
33. Higham, N.: Computing the Polar Decomposition—with Applications. SIAM Journal on Scientific and Statistical Computing. vol. 7, no. 4, pp. 1160-1174 (1995). doi:10.1137/0907079
34. Dubrulle, A.: An Optimum Iteration for the Matrix Polar Decomposition In: Electronic Transactions on Numerical Analysis (2001). vol. 8, pp. 21-25. (2001).